한국소성가공학회지 제 5 권 제 4 호, pp. 343~352, 1996

〈논 문〉

Further Development of Vision-Based Strain Measurement Methods to Verify Finite Element Analyses

Hyung Jong Kim* and Daeyong Lee**

(Received October 2, 1996)

Abstract

One of the preferred methods that can be used to verify the results of finite element analysis is to measure surface strains of the deformed part for the purpose of direct comparison with simulation results. Instead of using the usual manual method, the vision-based measurement method is capable of determining surface geometry and strain from the deformed grid pattern automatically with the help of a computer. To obtain strain distribution over an area, the coordinates of such a surface grid are determined from the multiple video images by applying the photogrammetry principle. Methods to improve the overall accuracy of the vision-based strain measurement system are explored and the possible accuracies that can be attained by such a measurement method are discussed. A major emphasis is placed on the initial grid application method, its accuracy, and ease of subsequent image processing. Finite element analyses of limiting dome height(LDH) test are carried out and the results of them are compared with experimental data.

Key Words: Vision-Based Strain Measurement Method, Grid Application, Limiting Dome Height(LDH) Test, Image Processing, Finite Element Analysis

1. Introduction

Numerical simulation of metal forming processes, such as by the finite element analysis method, is becoming a widely used analysis and predictive tool. Because of inherent approximations that are used in the analysis and uncertainty in some input parameters, it is often desirable to validate the results obtained by these simulation methods. A common practice to validate simulation results is to compare strain or stress obtained from both analysis and experiment. A simple loading condition with known solutions can be also used for validation purposes. In sheet forming, one of the best parameters to compare between the theory and experiment is displacement field or strain distribution.

An improved experimental method that can be used to determine surface geometry and strain distribution of deformed sheet metal is described. In essence, the procedure consists of acquiring several views of an object, digitizing in two dimensions using an automated vision system, corresponding points identified, and determining the 3-D coordinates of intersecting points from the relationship between the views. The position of the camera while taking the photographs is determined by encoders. These 2-D points from the photographs are used along with the camera posi-

*Department of Mechanical Engineering, Kangwon National University

**Department of Mechanical Engineering, Rensselaer Polytechnic Institute, Troy, NY, USA

tions to triangulate the 3-D coordinates of the surface area. Strains are computed in each triangular region while assuming pure homogeneous deformation in each triangle. Compared to other conventional strain measurement methods, the improved system described here produces hundreds of strain values over a significant region of a part in a short time.

The resulting accuracy of the strain measurement system is dependent on several factors : camera resolution, camera position resolution, internal camera geometry, the number of photographs used in determining the 3-D coordinates, the accuracy of the initial grid pattern, etc. Among these factors, an important parameter that has a significant influence on the final outcome is the accuracy of the initial grid in the undeformed configuration. The contrast and resolution of the initial grid also has a major effect on the total time required for image processing. For this reason, different methods of preparing square grids have been explored in the present work. The measurement accuracy is evaluated, and a comparison is made between differently prepared sheet samples. Advantages of certain grid preparation methods with regard to measurement accuracy and ease of image processing are discussed.

Finite element analyses of limiting dome height (LDH) test using a commercial code LS-DYNA3D are also carried out. The results of strain distribution under various conditions for friction coefficient and clamping force are analysed and compared with the corresponding experimental data.

2. Description of the Measurement Method

Several steps are required to make a video-based strain measurement of a sheet metal part. The first step is the application of a uniform square grid pattern to a sheet metal blank before it is deformed. Different grid patterns can also be used. Once the sheet has been formed into the final shape, a minimum of two photographs of an area are obtained by a video camera, and the intersecting grid lines on the surface of the part are located by a computer using automatic image processing

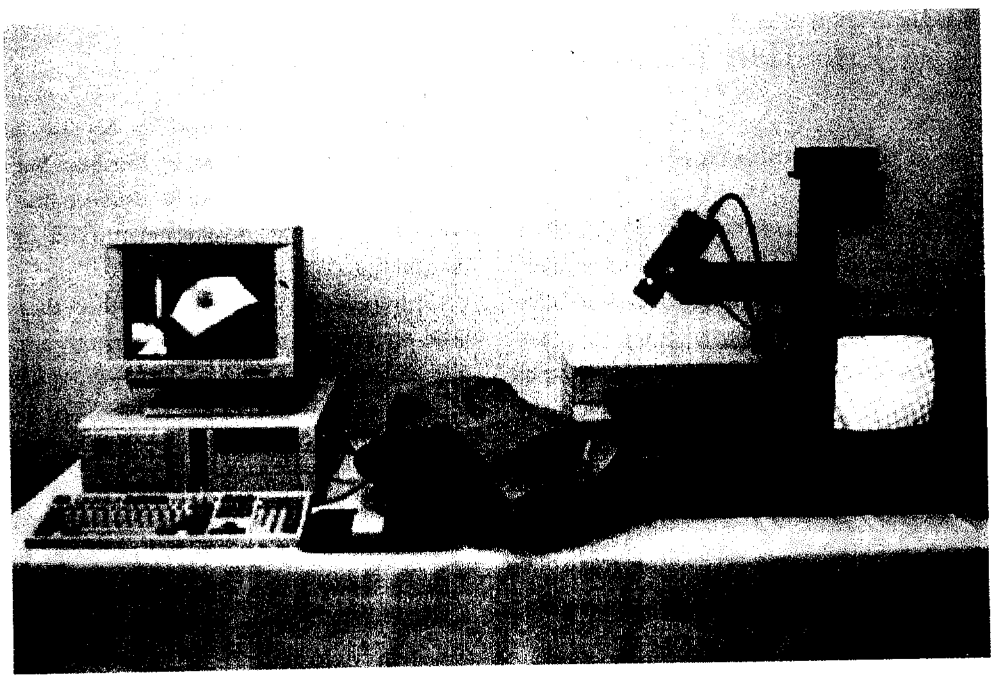

Fig. 1 A table model of vision based strain measurement system

of a digital representation of the image. The three-dimensional geometry is computed from the minimum of two sets of coordinate pairs and the geometrical relationship between the two views[1~6]. The surface strain components are calculated from the three-dimensional geometry based on the fact that it started as a flat undeformed grid of known size.

There are several different ways to acquire two or more views of an object to determine surface coordinates, as outlined in the previous papers[4~8]. In the present work, a Table Model as shown in Fig. 1 is used for the measurement purposes. A single camera of known position is mounted on a positioning frame and the object to be measured is placed on a rotating table as shown. Any number of photographs may be taken from different locations by turning the table or moving the camera. Encoders record the position of the table and the camera at the time a photograph is taken.

3. Experimental Procedure

3.1 Grid Preparation

In order to vary grid size accuracy, grid contrast and resolution, four different methods of grid preparation are used, as described below. Most of the grids have a spacing of 3/16 inch (4.763 mm), and a few of them have 2.00 mm spacing.

(a) Electro-Etching Method - A standard square grid stencil is prepared from the computer-generated positive films made from both 600 dpi (dots per inch) and 2400 dpi printers. Then, using an approprate chemical on the stencil which is placed on the top of sheet metal, an electric potential is applied on the metal surface. Square grids

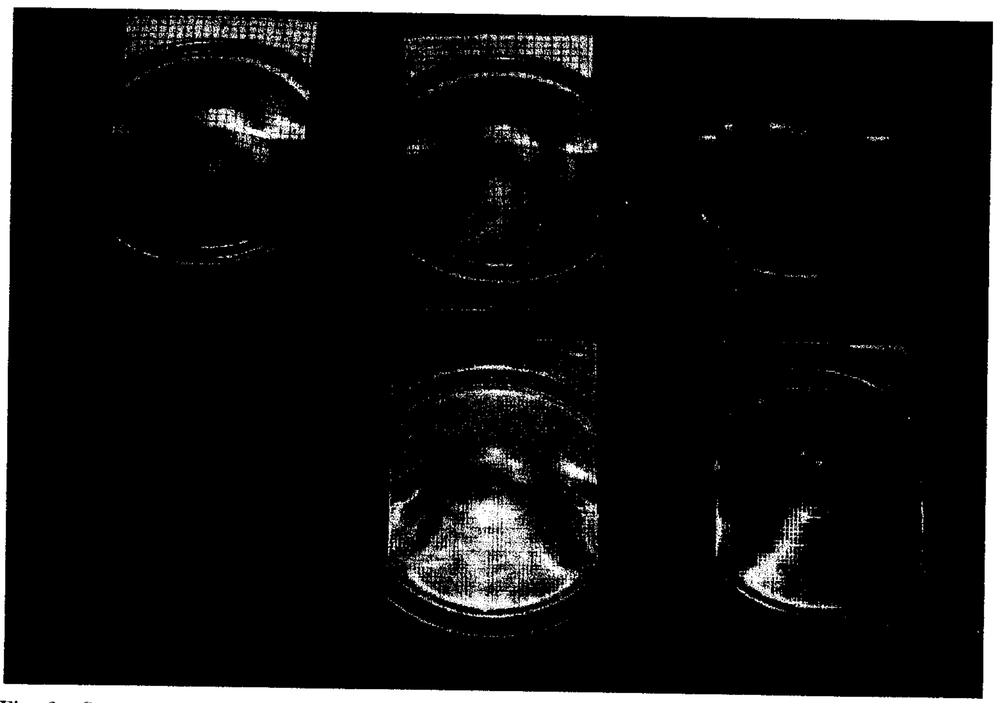

Fig. 2 Several deformed and undeformed sheet material parts prepared by different gridding methods : (a) 4.763 mm grid by electro-chemical method, (b) 4.763 mm grid by photo-emulsion method, (c) 4.763 mm grid by silk-screening method on polycarbonate sheet, (d) 4.763 mm grid by laser-etching method (undeformed), (e) 2 mm grid by photo-emulsion method using a positive film, and (f) 2 mm grid by photo-emulsion method using a negative film.

are lightly etched on the surface of sheet metal.

(b) Photo-Emulsion Method - A silver-halide emulsion used for coating photographic papers is applied. The aluminum sheet is cleaned, degreased, and a pre-coat of an oil-based glossy polyurethane is applied before a thin layer of the emulsion is placed. After the surface is dried, light is exposed through the positive film with the specially prepared grid and processed as with black and white photographs, all in the dark-room. Two positive films with square grids are used; one prepared with 600 dpi printer and the other with 2400 dpi printer.

(c) Silk-Screening Method - As in the electro-etching method, a stencil with desired square grid is prepared, mounted in a wooden frame evenly stretched in all four directions, and a suitably colored ink is applied to the metal surface with a sqeeze.

(d) Laser Etching Method - With a numerically controlled machine, a tool path for the square grid is specified and a relatively shallow groove is machined on the surface of sheet metal. The laser was applied at 25 KHz with 80% capacity and travelled at the speed of 100 mm/s.

3.2 Sheet Forming Experiments

LDH experiments were made using the MTS sheet formability testing system with the 101.6 mm diameter circular punch. The punch speed was 0.15 mm/s and the total displacement was 20.0mm. Representative deformed sheet samples with initial dimensions of 180 mm by 100mm are shown in Fig. 2 for 6111-T4 aluminum sheets prepared with different grid application method.

4. Grid Error and Measurement Results

4.1 Measurement Error Sources

Grid error can be determined by both analytical and experimental methods. The recently developed analytical photogrammetric measurement simulation program uses four accuracy parameters : one for photograph resolution, a second for camera positioning accuracy, a third for camera orientation accuracy, and a fourth for initial grid accuracy[7]. This information is used by the program to produce a set of data points, which are then used to produce a set of simulated photographs. To make a simulated photograph of the specified resolution, each coordinate of each point is adjusted by a random amount. The result of this is an even distribution of the pixel coordinate within the specified accuracy. This corresponds to locating a point within the photograph to either a one pixel accuracy from a camera with 1000 pixels across, or to a 1/2 pixel accuracy from a camera with 500 pixels across. Detailed results obtained from these simulations are reported in other papers[7,8].

A grid pattern is commonly applied to a sheet metal blank using an electro-chemical etching or photo-emulsion deposition processes. These grid patterns are commonly produced from an initial pattern printed from a computer. Typical printing resolutions vary from 300 dpi (dots per inch) to above 2400 dpi. In the past work, an initial grid size of 5mm was used, with each photograph having 20 grid squares across the image. The simulations showed that there is a significant measurement error with 300 dpi grids. A simulation was also made for 2400 dpi grids, and these results were close to those obtained using an ideally perfect grid.

Several square grids were produced and measured to test the accuracy of undeformed grids. These grids were composed of a set of squares of known size (3/16 in or 4.763 mm) to test the accuracy of the initial undeformed grid. Ideally, the computed strain should be equal to zero for the undeformed blank sheet. The measured strains were compared to the expected value of strain computed from a selected area. An area equal to 15 by 15 squares was measured at least about 100 times. Five sets of measurements have been made. One measurement was made with a 600 dpi grid and the other with a 2400 dpi grid and prepared by both electro-chemical and photo-emulsion method, respectively. Measurements were made by taking different numbers of photographs, using all quantities between 2 and 20 photographs. The measured error corresponding to 3 times the standard deviation equivalent values are shown in Fig. 3. For the 600 dpi grid, errors are considerably larger than those using the 2400 dpi grid. For the 2400 dpi grids, the results between two different preparation methods are similar.

4.2 Additional Experimental Results

Strain distributions of several LDH tested samples with different grid preparation methods have been determined using the automated video method shown in Fig. 1. In all cases, only one half of the deformed sheet metal part with the one side of the lock-bead area was examined for sheets with both 2 mm and 4.763mm square grids. For the case of grids with 2mm spacing, one quarter section of the formed part was actually measured. Typical results showing the actual measurement of the one half sections of the deformed part for the photo-emulsion prepared sample are shown in Fig. 4(a) and 4(b). The peak major strain obtained from the 2 mm grid, Fig. 4(a), is slightly higher than that obtained from the 4.763 mm grid, Fig. 4(b). The main cause for that difference is that

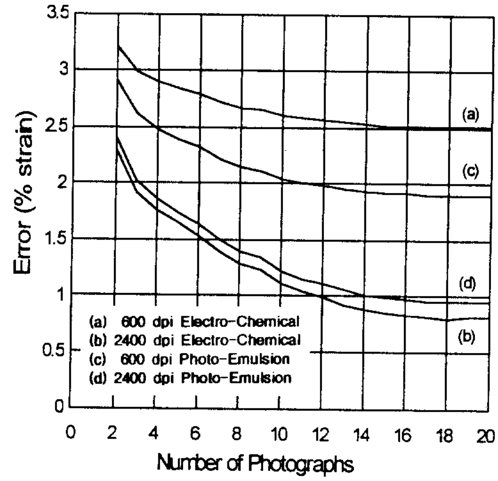

Fig. 3 Experimental error measured for differently prepared samples with increasing numbers of photographs and differnt grid qualities

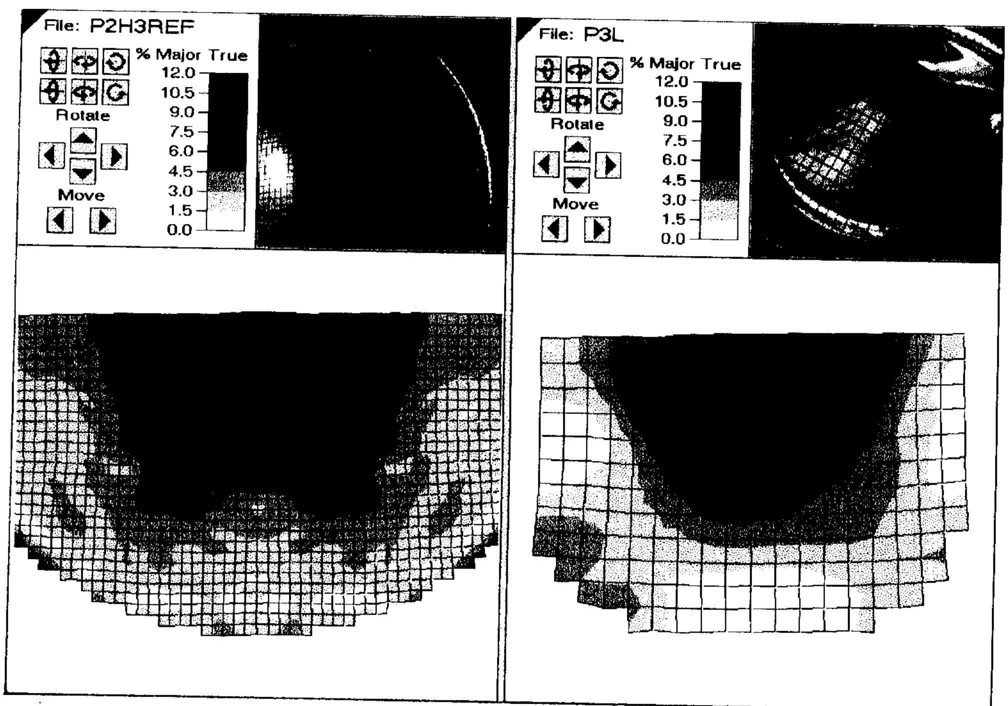

(a) 2mm grid (b) 4.763mm grid

Fig. 4 The experimentally measured major strain distribution of the deformed part for the photo-emulsion prepared samples the measured strains are always averaged over an distance, and this tends to yield higher peak strain values for samples with smaller grids.

5. Finite Element Analyses

A finite element simulation of LDH test was carried out using the PC version of a commercial finite element analysis code called LS-DYNA3D, Version 936[9], which is based on an explicit time integration scheme. An explicit code is inherently unsuitable for static or quasi-static problems such as in slow speed metal forming processes because it requires a very small time step to ensure stable convergence and reliable result. Therefore, it would be necessary to input a forming rate much higher than used in actual experiment within the limits of the rate that might produce negligible inertia effect. In the present analysis, the punch speed was assumed to be 5 m/s while it was actually 0.15 mm/s. Such an assumption is justified for 6111-T4 aluminium alloy because the flow strength of this alloy is basically insensitive to changes in strain rate.

The finite element model for simulation of LDH test is shown in Fig. 5. A quarter of the blank was subdivided into 1,125 4-node quadrilateral shell elements. The normal anisotropic elastic-plastic model was used for blank material, and some of the properties used are : Young's modulus $E=70.4$ GPa, Poison's ratio $\nu=0.26$, yield stress $\sigma_y=153$ MPa, anisotropic parameter $R=0.583$ and stress-strain curve $\sigma=558\varepsilon^{0.281}$MPa. The Coulomb friction coefficient, μ, was assumed to be 0.2 between blank and punch, and 0.3 between blank and clamping dies. Additionally, friction sensitivity analyses covering a wide range of friction coefficients from 0.0 to 0.3 for blank-punch interface were carried out. Clamping force of 100 kN was assumed to be applied by the upper clamping die to form a bead to prevent inward metal flow while the lower clamping die was fixed. And the clamping bead behavior was examined by assuming different sheet blank-draw bead interaction model.

In Fig. 6, the input curves for punch advancement and clamping force applied on the upper die as functions of time are displayed, and the corresponding time-displacement results for the center of dome, O, the edge point, E, and the upper clamping die are also plotted. Small oscilations that have been observed in the displacement curves for two pre-selected points on the blank during clamping porcess(time<5ms) seem to be due to dynamic response. However, they seem to disappear during

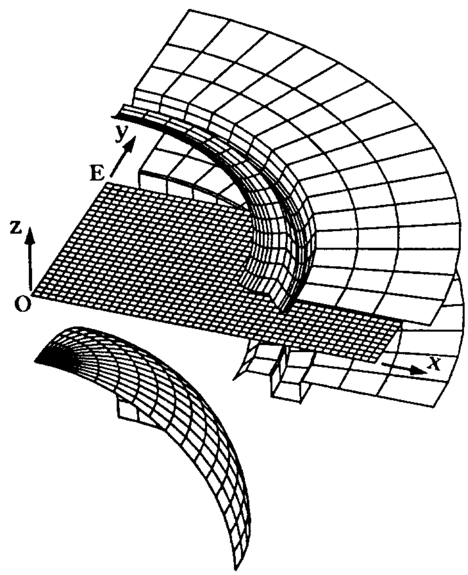

Fig. 5 A quarter model for finite element simulation of LDH test

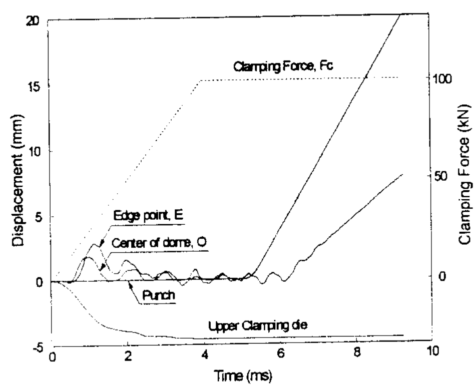

Fig. 6 Input curves for punch advancement and clamping force, and the corresponding time-displacement results for selected nodal points

the dome forming process ; therefore, it is assumed that dynamic effect does not influence significantly the computed strain distribution.

The results of friction sensitivity analyses are shown in Fig. 7. It is demonstrated that frictional conditions between blank and punch affect the level of strain but does not change the location of the peak strain. This result may be compared with the well-known case of axisymmetric punch stretching where the peak strain position moves away from the center of dome as friction coefficient increases.

All the different forming conditions used in the sensitivity analyses are summarized in Table 1 in terms of the peak major strain and its location (distance from center of dome along x-axis). Friction coefficient between blank and punch, μ_p was varied from 0.0 to 0.3. Other forming conditions used in the simulation study were related to modeling methods of clamping condition ; which were (a) various clamping force (F_c=50kN, F_c=100kN and F_c=200kN), (b) prescribed displacement of clamping die instead of clamping force (δ_c=4.55mm) and (c) simplified boundary conditions without bead (rectangular blank and circular-cut blank). In the case of (c), all nodal points on the boundary were assumed to be fixed. The experimentally observed result is also included in the table. It is shown that the magnitude of clamping force within reasonable range in with-bead analyses does not affect the level and the location of peak major strain as much as friction condition does. Peak strains of without-bead analyses are 1.5-2.0% less than those of with-bead analyses. These differences may be mainly due to pre-strain which occurs over the area enclosed with bead during clamping process.

The computed strain distributions under the selected forming conditions are summarized in Fig. 8. Minor changes in strain distributions are observed under these forming conditions.

The result of computed major strain distribution for the LDH formed part at punch displacement of 20 mm is compared with the corresponding experi-

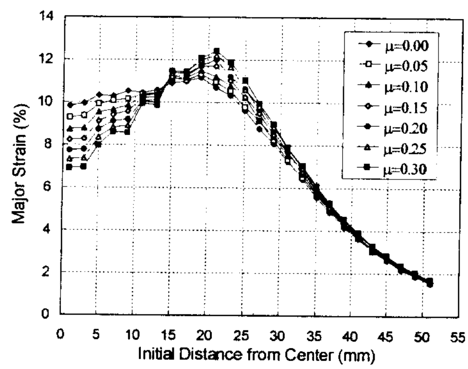

Fig. 7 Distributions of major strain under different assumed friction coefficients

Table 1 Computed and experimental peak major strain and its location

Cond.	With Bead				Without Bead		Experiment
μ_p	F_c=50kN	F_c=100kN	F_c=200kN	δ_c=4.55mm	Rectangular	Circular-cut	
0.00		11.0(18)					
0.05		11.2(18)					
0.10		11.4(20)					
0.15		11.7(20)					
0.20	11.5(20)*	11.9(20)	12.1(20)	11.9(20)	9.5(20)	9.0(18)	12.4(13)
0.25		12.1(20)					
0.30		12.3(20)					

*Peak major strain in % (Initial distance from center to peak location in mm)

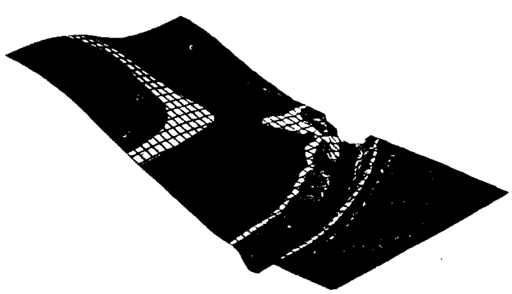

(a) $F_c=100kN$, $\mu_p=0.1$

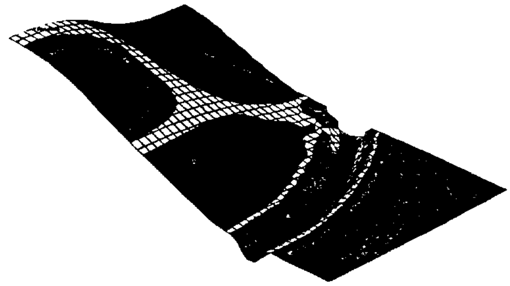

(c) $F_c=100kN$, $\mu_p=0.3$

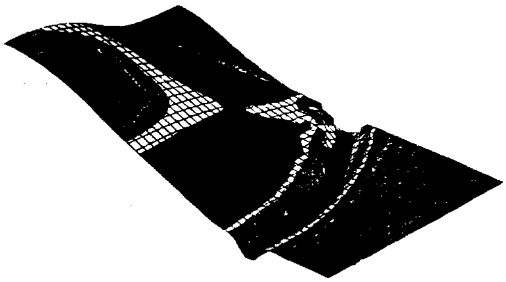

(b) $F_c=100kN$, $\mu_p=0.2$

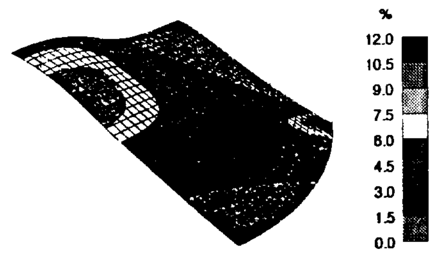

(d) Circular-cut blank without bead, $\mu_p=0.2$

Fig. 8 Distributions of major strain under the selected forming conditions

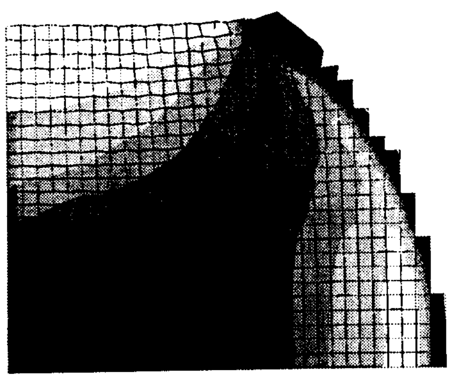

(a) FEA

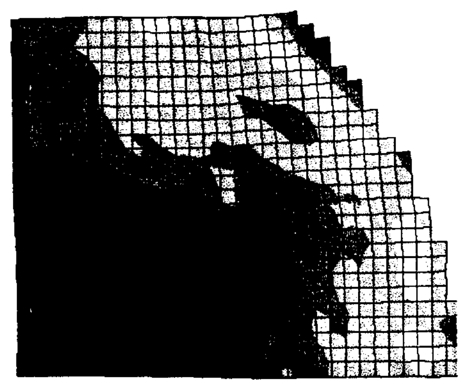

(b) Experiment

Fig. 9 Results of major strain distributions for the LDH formed part

mental result in Fig. 9. It shows that computed data have similar trends with experimental data except the region around the clamping bead. In particular, the computed peak major strain is almost identical to that of experimental results although the position of peak strain is further shifted away from the center for the simulation result.

6. Summary and Conclusions

Accuracy of the strain measurement is dependent on initial conditions and many process parameters. Some of these parameters are photograph resolution, camera positioning resolution, the number of photographs taken, internal camera geometry, the initial grid quality, etc. One of the relatively easy parameters to adjust is the accuracy and resolution of the initial undeformed grid. The accuracy of line spacing affects the accuracy in strain measurement and the resolution as well as the overall quality of the grid influence the image processing time. For that reason, four different grid preparation methods as well as the printing quality of computer generated grid pattern have been examined in this work.

Electro-chemical and photo-emulsion methods provide a acceptable and comparable accuracy if the printer resolution is at least 2400dpi. The silk-screening method uses a dried paint and has limited stretching capability. All of these methods have one important deficiency that additional error is introduced during the subsequent grid preparation steps, such as wrinkling of the stencil, non-uniform contact of the gridded film and metal surface. The laser-etching method does not require additional processing of the original negative film, and is the preferred grid preparation method, provided that sufficiently large area can be readily gridded and the overall cost is reasonable.

Accuracies are improved by increasing the number of photographs, the photograph resolution, the positioning resolution, and the grid accuracy, all at the same time. The current measurement method can be improved to achieve an accuracy of about ±1.5% true strain, provided the original grid is made to about 0.5% accuracy, other parameters selected at optimum conditions, and several photographs are taken for the sample area to be measured.

Strain distribution obtained by finite element analysis using LS-DYNA3D has similar trend to experimental result. In particular, the computed peak major strain is almost equal to measured peak strain although the position of peak strain for the simulation result is further shifted away from the center of the dome.

It seems that frictional condition between blank and punch in LDH test has an influence on the strain level but does not affect the location of the peak strain so much. The magnitude of clamping force does not change the level and location of peak strain. Simplified models without bead gave much less peak major strain than experiment or actual models with bead. This result says an excessive simplification of boundary condition in finite element analysis may sometimes yield a significant error.

Acknowledgements

David Manthey prepared many of the figures including the error analysis results (Fig. 3) and Rebecca Pearce provided assistance in the manuscript preparation. Jerry Moleski of GM Research Laboratory provided laser-etched grid samples.

References

(1) Bednarski, T., 1977, "Application of Stereo-photogrammatic Methods to Analyze Kinematics and Dynamics of Shells" (in Polish), Warszawa, pp. 25~160.

(2) Sowerby, R., J. L. Duncan, and E. Chu, 1986, "The Modelling of Sheet Metal Stampings", International Journal of Mechanical Science, Vol 28, pp. 415~430.

(3) Schedin, E. and A. Melander, 1986, "The Evaluation of Large Strains from Industrial Sheet Metal Stampings with a Square Grid", Journal of Applied Metalworking, Vol 4, pp. 143~156.

(4) J. H. Vogel and D. Lee, 1990, "The Automated Measurement of Strains from Three-Dimensional Deformed Surfaces", Journal of Metals, Vol. 42, pp. 8~13.

(5) M. I. Kapij, J. Moleski, T. Ohwue, J. H. Vogel, and D. Lee, 1992, "Comparison of Different Surface Strain Measurement Methods Used for Deformed Sheet Metal Parts", Society of Automotive Engineers Automotive Stamping Applications and Analysis SP-897, pp. 73~85.

(6) Manthey, D. W., R. M. Bassette, and D. Lee, 1993, "Comparison of Different Surface Strain Measurement Techniques Used for Stamped

Sheet Metal Parts", Proceedings of International Body Engineering Conference : Body Assembly & Manufacturing, September 21-23, pp. 106~111.

(7) Manthey, D. W. and D. Lee, 1995, "Recent Developments in a Vision-Based Surface Strain Measurement System", Journal of Metals, Vol. 47, pp. 46~49.

(8) Manthey, D. W. and D. Lee, 1995, "A Portable, Non-Contact Coordinate and Strain Measuring Machine", Proceedings of International Body Engineering Conference : Advanced Technologies and Processes, October 31-November 2, pp. 152~162.

(9) Livermore Software Technology Corp., 1995, "LS-DYNA3D Users' Manual".